Chemical Engineering Journal 501 (2024) 157754

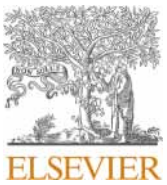

Contents lists available at ScienceDirect

Chemical Engineering Journal

journal homepage: www.elsevier.com/locate/cej

Contact-electro-luminescence triggered by triboelectric charge

Chong Xu [a,b], Shaoxin Li [a,b], Zhe Yang [a,b], Morten Willatzen [a,b], Zhong Lin Wang [a,c,d,*], Di Wei [a,e,*]

[a] Beijing Institute of Nanoenergy and Nanosystems, Chinese Academy of Sciences, Beijing 101400, PR China
[b] School of Nanoscience and Engineering, University of Chinese Academy of Sciences, Beijing 100049, PR China
[c] Beijing Key Laboratory of Micro-Nano Energy and Sensor, Center for High-Entropy Energy and Systems, Beijing Institute of Nanoenergy and Nanosystems, Chinese Academy of Sciences, Beijing 101400, PR China
[d] Georgia Institute of Technology, Atlanta, GA 30332-0245, United States
[e] Centre for Photonic Devices and Sensors, University of Cambridge, 9 JJ Thomson Avenue, Cambridge, CB3 0FA, UK

ARTICLE INFO

Keywords:
Contact-electro-luminescence
Triboelectric charge
Reactive oxygen species
Intermediate state
Luminol

ABSTRACT

Luminol, a prominent chemiluminescent reagent, is extensively employed in biochemical and environmental analyses for its ability to produce rapid luminescence through oxidation in aqueous solutions. However, the lack of comprehensive studies on the observation and regulation of intermediate species during this luminescent reaction may limit its effectiveness in detection applications. Understanding these intermediates is crucial for enhancing the accuracy and reliability of luminol-based detection methods. To solve the above problems, this work proposes a straightforward and effective approach to directly oxidize luminol via reactive oxygen species (ROS) generated from contact electrification (CE) between inert solid dielectrics and deionized (DI) water, termed contact-electro-luminescence (CEL). Metal-free, cost-effective solid dielectrics present a promising alternative to expensive metal-based catalysts, aligning well with the principles of green chemistry and sustainable development. In such reaction system, ROS can be regulated by various solid dielectrics and additives (such as xylitol and p-benzoquinone), thereby tuning the luminol reaction. More importantly, two distinct luminescent emission peaks are directly observed and the intensity of the emission peaks of the two intermediate states can be regulated. The observation of intermediate is beneficial to reveal the intrinsic of luminescence reactions, exploiting the effective and tunable luminescence system. Moreover, CEL provides a new mechanical-photonic conversion paradigm to study luminol luminescence via triboelectric charge from the CE effect. CEL can offer distinct characteristic signals, offering potential applications in high-efficiency and specific detection for environmental monitoring, biomedical diagnosis and food safety testing etc.

1. Introduction

Luminol, with its distinctive chemiluminescent properties, is pivotal in various applications such as medical diagnostics, biological analysis, and environmental monitoring [1,2]. With the ongoing advancement of scientific technology, the utility of luminol is expected to expand further. Its chemiluminescent properties facilitate high-resolution monitoring, while its fluorescence characteristics provide a basis for investigating its luminescence mechanisms. Generally, luminol reacts with reactive oxygen species (ROS), such as hydroxyl (•OH) radicals, to produce 3-aminophthalate (3-APA) and its associated excited state. Blue light is emitted when this excited state returns to the ground state. However, unless oxidized •OH radicals are rapidly generated ($<10^{-4}$ s) in high concentrations ($>10^{-7}$ mol/L), almost no light will be detected [3]. Such rapid reaction poses a challenge for investigating the specific luminescence mechanism of luminol, making it particularly difficult to detect the immediate reactants that is essential in determining the accuracy of detection. By observing the intermediate process of the luminol luminescence reaction in a slow and controllable manner and regulating the luminescence peaks, more substances reacting with luminol can be detected. This enhances detection accuracy and broaden the detection range. To date, numerous efforts have been made to capture intermediates and elucidate the mechanisms of luminol luminescence, primarily through electrochemical luminescence methods such as cyclic voltammetry (CV) and differential pulse voltammetry (DPV) [4]. However, these methodologies primarily rely on the optimal match

* Corresponding authors at: Beijing Institute of Nanoenergy and Nanosystems, Chinese Academy of Sciences, Beijing 101400, PR China.
E-mail addresses: zhong.wang@mse.gatech.edu (Z. Lin Wang), dw344@cam.ac.uk (D. Wei).

https://doi.org/10.1016/j.cej.2024.157754
Received 27 July 2024; Received in revised form 31 October 2024; Accepted 16 November 2024
Available online 17 November 2024
1385-8947/© 2024 Elsevier B.V. All rights are reserved, including those for text and data mining, AI training, and similar technologies.

between electroactive materials and the electrolyte solution. They are also closely related to the appropriate choice of the electrochemical window; otherwise, side reactions may occur, interfering with the elucidation of the luminol reaction pathway. Although electrochemical luminescence methods can modulate charge, they are constrained by electrochemical window compatibility and the need for electroactive materials. Moreover, the system's complexity and rapid reaction dynamics impede clear, controllable analysis of intermediate states.

Mechanochemistry has been widely employed to initiate luminescence reactions through external mechanical stimulation. Mechanoluminescence (ML) is a unique light-emitting phenomenon that can be excited by squeezing, impact, or even ultrasonication (US) [5]. ML not only reduces dependence on traditional electrical energy, aligning with the principles of green chemistry, but also minimizes side reactions within a more streamlined reaction system, facilitating the investigation of basic reaction mechanisms [6]. It is thus believed that ML has extensive applications in luminescence switches, mechanical sensors, optoelectronic products etc. [7] Generally, ML can be classified into various luminescent modalities such as sonoluminescence (SL), Piezoluminescence (PL), triboluminescence (TL), triboelectrification-induced electroluminescence (TIEL) etc. SL describes the emission of light from the collapse of a small gas bubble in a liquid solution due to the cavitation effect, where significant thermal energy is released, resulting in a weak light flash [8–10]. PL and TL typically occur with material deformation, distortion, or cracking under strong mechanical forces, based on the piezoelectric effect or friction [11–14]. Additionally, charge separation and recombination at the interface of solid–solid triboelectrification can also induce luminescence, classified as TIEL [15]. However, the practical application of these modalities is constrained by the weak and uncontrollable mechanical strength of solid luminescent materials, which complicates the investigation of their luminescent mechanisms. Furthermore, these ML approaches are infrequently employed in luminol reactions, which require a substantial concentration of ROS in solution. Recently, the intriguing concept of contact-electro-catalysis (CEC) has garnered significant attention in green chemistry, leveraging the contact electrification (CE) effect. It is well known that electron transfer and subsequent radical generation, such as •OH, superoxide ($\bullet O_2^-$), and singlet oxygen ($^1O_2$) radicals, can drive chemical reactions. CEC holds great potential for applications in pollutant degradation, hydrogen peroxide synthesis, and recycling of used cathode materials due to its sustainable non-metal dielectrics capability and the extensive selection of materials under mild conditions [16–20]. Metal-free, cost-effective solid dielectrics present a promising alternative to expensive metal-based catalysts, aligning well with the principles of green chemistry and sustainable development. Furthermore, a unified framework integrating the concepts of work functions, electronegativity in the triboelectric series, and standard electrode potentials has been developed based on electron transfer capabilities, introducing the concept of contact-electro-chemistry (CE-Chemistry) [21]. This promising technique represents a green and sustainable approach for various chemical reactions, including the redox reactions of ferrocene and the polymerization of conducting polymers.

To address the challenge of establishing a pure luminol reaction system, complicating the investigation of intermediates, this work proposes a simplified luminol reaction system. Leveraging the CE effect, contact-electro-luminescence (CEL) facilitates the direct observation and regulation of luminol intermediates. In particular, an inert solid dielectric of fluorinated ethylene propylene (FEP), when in contact with deionized (DI) water, induces the generation of ROS that initiate the ring-opening reaction of luminol. Unlike traditional chemical catalysis, the catalyst in CEL is inherently inert, primarily facilitating interfacial electron transfer to initiate ROS generation and subsequent reactions. This reduces the background interference of side reactions in the luminol reaction process. Moreover, these inert solid dielectrics offer broad versatility, and the widespread CE effect highlights the universality of CEL. Electron paramagnetic resonance (EPR) analysis confirmed the presence of ROS in CEL, whose generation is associated with the electrostatic charge from the adjustable CE performance. More importantly, introducing certain aqueous additives in luminol CEL enabled the direct observation and regulation of luminol-related intermediates at two distinct luminescence peaks at 425 nm and 475 nm. In the future, CEL can be further integrated with spectroscopy or mass spectrometry devices for real-time monitoring and rapid analysis of luminescence mechanisms. This work not only introduces a straightforward approach to study luminol luminescence reactions but also lays the groundwork for integrating CE-Chemistry across diverse fields such as high-efficiency and specific detection for environmental monitoring, biomedical diagnosis and food safety testing etc.

2. Material and methods

2.1. Reagents and materials

Luminol [$C_8H_7N_3O_2$, Macklin 98 %], NaOH [Macklin 99.5 %], p-benzoquinone [$C_6H_4O_2$, Macklin 99.5 %], erythritol [$C_4H_{10}O_4$, Aladdin, 99 %], xylitol [$C_5H_{12}O_5$, Aladdin, 99 %], sorbitol [$C_6H_{14}O_6$, Aladdin, 99.5 %], 5,5-dimethyl-1-pyrroline N-oxide [DMPO, Dojindo], 2,2,6,6-tetramethyl-4-piperidone [TEMP, Dojindo], potassium ferricyanide [$K_4[Fe(CN)_6]$, HengXing, Analytical Reagent], fluorinated ethylene propylene (FEP) [Dupont], polytetrafluoroethylene (PTFE) [Dupont].

2.2. Sample preparation

A 4.0 mL sample solution containing 2.0 mM luminol and 30.0 mM NaOH was prepared in advance, about 10.0 cm × 30.0 cm solid dielectric film was cut into 0.5 cm × 1.0 cm pieces and then put into the solution sample. An ultrasonic bath (VGT-190D, 40 kHz, 360 W) was used to promote the CEL. The temperature in the ultrasonic bath was regulated to a constant temperature of 40 ℃. The solution of xylitol was prepared by adding 0.15215 g of xylitol in 10 mL DI water, achieving 0.1 M. The mix solution of the best luminous intensity was prepared by adding 16 μL 0.1 M xylitol solution and 0.1728 mg of p-benzoquinone into 3.984 mL DI water. The dielectric materials after reactions were taken out by using plastic tweezers, then dried in an oven at 40 ℃ overnight before analysis. Samples for EPR analysis were prepared with 4.0 mL of DI water US with FEP fragments about the total size of 10.0 cm × 30.0 cm.

2.3. Sample characterization

Fluorescence spectrometer (Edinburgh Instruments, full-featured, FLS980-S2S2-stm) was used to test luminol luminescence intensity, using $\lambda_{excitation} = 375.0$ nm. The UV–Vis absorptions of the samples were measured by UV–Vis spectrometer in a range of 200.0–600.0 nm. Electron paramagnetic resonance (EPR) was recorded on a Bruker EMX plus-9.5/12/P/L. The measurements were conducted in X-Band (9.830243 GHz), with amplitude modulation of 1 G, microwave power of 2 mW, an amplitude modulation frequency of 100 kHz, conversion time of 60.00 ms, and a time constant at 40.96 ms. Morphologies of FEP films were observed by the scanning electron microscope (SEM SU8020, Hitachi). The Energy Dispersive X-Ray analysis (EDX) was conducted on FEI Nova 450 equipped with an AMETEK Octane Super appendix. The chemical states of dielectric materials before/after the CEL were measured by near atmospheric pressure X-ray photoelectron spectrometer (NAP-XPS, SPECS, Germany). FTIR analysis was conducted on a Bruker Vertex 80 v on a range from 400 to 3000 cm^{-1}. The high-performance liquid chromatography-mass spectrometry (HPLC-MS) analysis was conducted using a Thermo Scientific Q Exactive Orbitrap Quadrupole-Electrostatic Field Orbitrap High-Resolution Tandem Mass Spectrometer. The HESI ion source of the mass spectrometer was set at −3.0 kV, in positive ion mode. The mass spectrometry scanner was set on the full scan range of 100–1000 *m/z*. The resolution of the instrument is 70,000 FMHM. The

column used was a Hypersil Gold C18 (2.1 × 100 mm, 1.9 μm), the column temperature is set at 40°C. The injection volume is 5 μL. Mobile phase A is composed of 0.1 % formic acid aqueous solution, and mobile phase B is an acetonitrile solution. The parameters. used for Density Functional Theory (DFT) simulations are presented in Supplementary Note.

3. Results and discussion

3.1. The luminol CEL

In luminol solution, a controllable luminescence process is crucial for investigating reaction mechanisms and enabling highly sensitive detection for applications in environmental pollution, medical diagnosis, and food safety. This work proposed a new ML approach based on CE between solid dielectric and liquid, referred to CEL (**Fig. 1a**). A straightforward and controllable luminol luminescent reaction was realized by CEL, involving interfacial electron transfer of CE, instead of the mechanical forces that cause the materials deformation or cracking. Unlike luminol in traditional chemiluminescence (CL) systems, which relies on extremely active catalysts, such as hydrogen peroxide, Fe^{3+}, horseradish peroxidase, to rapidly oxidize to form 3-APA* (excited state), the emission of blue light with a luminescence wavelength of 425 nm occurs when 3-APA* returns to its ground state of 3-APA (**Fig. S1**). The solid dielectrics used in CEL is inherently inert, which avoids the use of heavy metal catalysts or organic solvents, making it more suitable for sustainable application. The preparation process for the original luminol solution, containing only luminol (2 mM) and NaOH solution (30 mM, 4 mL), is schematically illustrated in the left panel of Fig. 1**b**. Then the original luminol solution with shredded FEP films (total size: 10*30 cm^2) in bottle was transferred to an ultrasonic chamber as shown in the right panel of Fig. 1**b**. Ultrasonic waves produce cavitation in liquid media, leading to the growth and collapse of cavitation bubbles. Instantaneous rupture and collapse of cavitation bubbles facilitates the solid–liquid CE, which can induce chemical reactions. It was reported that US enhanced the electron transfer in CE between FEP and water, thereby generating the ROS [16]. Therefore, US was used as an important external-field modulation and mechanochemical method with superior spatiotemporal controllability to modulate the solid–liquid CE efficiency by ultrasound frequency, ultrasound duration, etc. Moreover, it is worth noted that the ROS generation process through CE is relative slow and insufficient to immediately induce luminol emission, providing an opportunity to detect the intermediate for studying the luminescence mechanism of luminol. Combined with the fluorescence spectra, as shown in Fig. 1**c**, the luminescence wavelength of original luminol solution is 425 nm. A subtle peak around 475 nm was observed in the luminol solution with FEP under ultrasonication, contrasting with the absence of this peak in the luminol solution without FEP, underscoring the critical role of inert dielectrics in CEL. This finding indicates that inert solid dielectrics indeed enhance the luminol reaction through solid–liquid CE, potentially generating specific intermediates. Nonetheless, luminol luminescence at 425 nm remained detectable even without inert dielectrics, likely due to ROS generation, suggesting a contribution from mechanochemical effects. Here, ultrasonication is employed solely as a mechanical facilitator for CE at the solid–liquid interface. Compared with the direct action of ultrasonication on reactants, CE between solid and liquid provides the possibility for controllable chemical reactions, showing a more exciting effect than

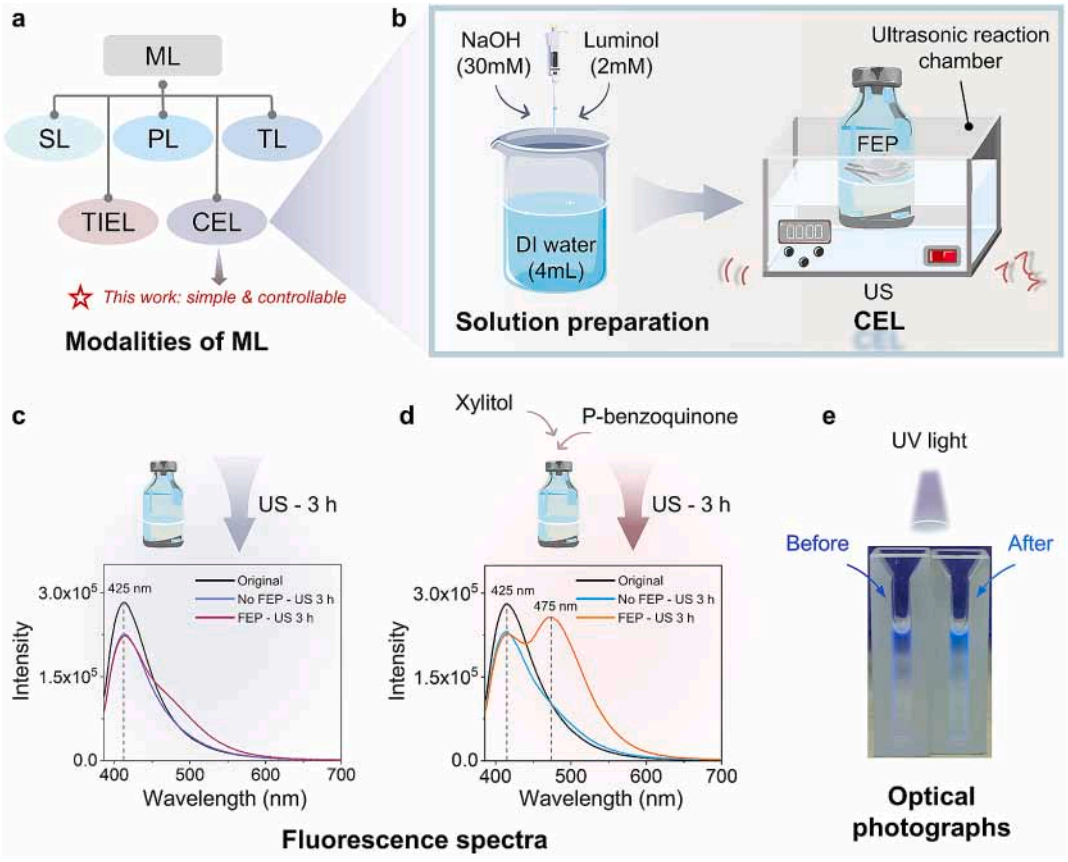

Fig. 1. Luminescence of luminol by contact-electro-luminescence (CEL). (a) Various luminescent modalities of mechanoluminescence (ML). (b) Schematic illustration of the experimental process. (c) The fluorescence spectra after 3 h of ultrasonic reaction without additives. (d) The fluorescence spectra after 3 h of ultrasonic reaction with xylitol and p-benzoquinone. The fluorescence spectra were all recorded at room temperature in a 1 cm quartz cuvette. (e) Optical photographs with emission in different colour of the luminol luminescence with additives before / after the CEL reaction under UV light illumination.

only through ultrasonic cavitation. To further investigate the luminol reaction process, additives such as xylitol and p-benzoquinone were introduced into original luminol solution. As shown in Fig. 1**d**, the luminescence peak at 475 nm was distinctly evident only in the luminol solution with FEP under US. This further underscored the CE between FEP and water facilitated the luminol reaction, and the additives indicated the operability of CEL. Moreover, no luminescence peaks at 425 nm or 475 nm were observed in pure additive solutions without luminol, even after 3 h of ultrasonication with FEP films (**Fig. S2**). This strongly suggests that these luminescence peaks are associated with luminol reaction products rather than new luminescent centers introduced by the dielectric. Furthermore, the luminescence photograph of the luminol-additive mixture after CEL process under UV exposure reveals a color variation compared to that observed without the CEL process (Fig. 1**e**). These results suggest that the oxidation reaction of luminol facilitated by CEL yields distinct products relative to the luminescence process of luminol in the absence of CEL [22]. **Fig. S3** illustrates the repeatability and stability of luminescence spectra at 425 nm and 475 nm, confirming robust consistency in the data.

3.2. Factors influencing CEL

It is well known that luminol is not soluble in DI water, therefore, it was dissolved in an aqueous NaOH solution (30 mM) in this work. As shown in Fig. 2**a**, the luminescence peak at 475 nm diminished as the concentration of NaOH increased. This indicated that excessive ionic concentration might impede electron transfer in solid–liquid CE due to the shielding effect of the interfacial electrical double layer (EDL), aligning with our previous results [21,23,24]. Studies have indicated that sugar alcohols, such as xylitol, exhibit notable CE performance [25], demonstrating potential for enhancing the triboelectric charge transfer in CEL reactions. The influence of various concentrations of xylitol on CEL was also investigated. As shown in Fig. 2**b**, an optimized concentration of 0.4 mM xylitol was favorable for observing the intermediates with luminescence peak of 475 nm. The high concentration of xylitol may inhibit further electron transfer and reactions during the CE process [21,23,24], as its positive hydration properties lead to the formation of a water layer [26]. Furthermore, it can be seen from **Fig. S4** that the optimized concentration of NaOH and xylitol in CEL for observing the intermediate is 30 mM and 0.4 mM, respectively. Erythritol and sorbitol were additionally selected to investigate the influence of sugar alcohols on CEL. While all three sugar alcohols serve as hydrogen bond donors through their hydroxyl groups, enhancing surface charge, they differ in spatial configuration and hydroxyl group numbers. Notably, xylitol exhibited distinct advantages in CEL, particularly in enabling the detection of intermediates, as evidenced by a luminescence peak at 475 nm, compared to erythritol and sorbitol. (Fig. 2**c**). In contrast, only one luminescence peak at 425 nm can be observed in the reaction solution with additives before the CEL reaction (**Fig. S5**). Moreover, **Fig. S6** shows that the three sugar alcohol additives have minimal impact on the acidity and alkalinity of the original luminol solution, with all solutions maintaining a pH of 12 at room temperature. This indicated that while sugar alcohol additives did not alter the reaction conditions of CEL, they might indeed affect the reaction process, for example, facilitating the generation of intermediates. It was reported that the occurrence of two emission peaks of luminol was attributed to the formation of two different kinds of excited state molecules: an excited aminophthalate ion (3-APA*) hydrogen bonded to water or protonated fully (emitting at 424 nm) [27], and a deprotonated 3-APA* (emitting at 485 nm) [28]. Therefore, it is reasonable to speculate that sugar alcohols will affect the formation of 3-APA* during CEL. Unlike erythritol and sorbitol, which exhibit negative hydration properties [29,30], xylitol, with its positive hydration characteristic [26], enhances the formation of hydrogen-bonded 3-APA*, thereby promoting the luminol emission peak at 475 nm. As illustrated in **Fig. S7**, the spatial conformations of these sugar alcohols show that xylitol tends to adopt a linear configuration in aqueous solution, increasing its binding affinity with water molecules. This interaction may weaken the luminol emission at 425 nm while enhancing the emission at 475 nm. To some extent, sugar alcohol additives will compete with reactants to consume ROS in solution [31],

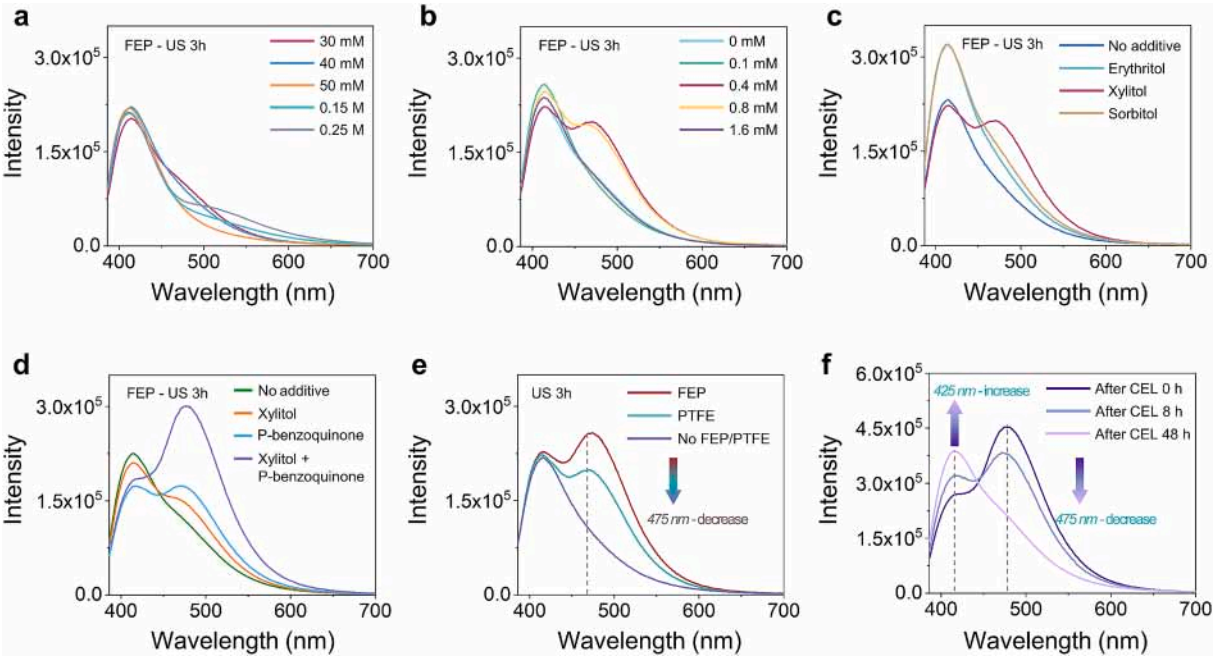

Fig. 2. Influence of factors in solution samples on contact-electro-luminescence (CEL). Luminescence intensity of luminol with different concentrations of (a) NaOH and (b) xylitol. The luminol CEL intensity decreases with increasing concentrations due to the shielding effect of electrical double layer (EDL). (c) CEL intensity with two other sugar alcohol additives, erythritol and sorbitol, and no additive, compared to the xylitol additive. (d) Fluorescence spectra with xylitol, p-benzoquinone, and xylitol and p-benzoquinone. (e) CEL with other dielectric materials, e.g., polytetrafluoroethylene (PTFE). (f) A decrease in luminescence emission intensity at 475 nm and an increase in luminescence intensity at 425 nm.

allowing for a slower and more controllable luminol reaction, which enables clear detection of luminol intermediates during CEL with an optimal concentration of xylitol. In order to investigate the possible generation of different free radicals in different atmospheres, potassium ferrocyanide (K_4 [$Fe(CN)_6$]) oxidation induced by CE-Chemistry was conducted. A similar phenomenon can be observed from UV–Vis spectra in the CE-oxidation of K_4 [$Fe(CN)_6$] (**Fig. S8a** and **Fig. S9a**). The concentration of the oxidized product, potassium ferricyanide (K_3 [$Fe(CN)_6$]), decreased when sugar alcohol was introduced into the CE-oxidation system, corresponding to the decrease in the absorbance intensity at 420 nm. Interestingly, this impact became less obvious when nitrogen (N_2) was passed through the reaction (**Fig. S8b** and **Fig. S9b**), indicating that the sugar alcohols primarily interact with radicals associated with oxygen (O_2). P-Benzoquinone is a common radical quencher that reacts with active free radicals, such as $\bullet O_2^-$ radicals. When p-benzoquinone (0.4 mM) was added to the CEL reaction system, the luminescence peak of the luminol intermediate could also be observed (the blue line in the Fig. 2**f**). When both xylitol and p-phenol were introduced at the same concentration, the luminescence peak of the luminol intermediate became more prominent (the purple line in the Fig. 2**f**). No luminescence peak was observed in the reaction solution without luminol (**Fig. S2**), indicating that the additives used in this work did not exhibit luminescence characteristics. Moreover, the luminescence peak at 475 nm did not appear in the reaction solutions before CEL (**Fig. S10a**) and was not prominent in the reaction solutions under US without FEP (**Fig. S10b**). These results suggested the critical role of CE between FEP and DI water in CEL reactions.

A more detailed analysis of the conditions affecting CEL were provided, including the impact of the size and thickness of the FEP film (**Fig. S11**), as well as ultrasonic power, duration, and temperature (**Fig. S12**). When the total area of the FEP film is the same, the effect of different sizes on the CEL is not particularly significant. Relatively, smaller sizes of FEP film may have a greater specific surface area of contacting with DI water, and therefore the CEL may be slightly better (**Fig. S11a**). The thinner the FEP film the better the CEL results, which may be attributed to the higher CE performance [32] (**Fig. S11b**). In our experiments, in addition to studying the effect of the size and thickness of the FEP film, we all have chosen to cut the FEP film into 0.5 * 1.0 cm^2, as well as 0.03 mm thickness.

Moreover, ultrasonic power we investigated the luminol CEL by FEP film under different ultrasonic powers of 500 W, 360 W, 120 W (**Fig. S12a**), and different ultrasonication time of 1 h, 3 h, 5 h (**Fig. S12b**), and different temperature of 20 ℃, 40 ℃ and 60 ℃ (**Fig. S12c**). The experimental results showed that the luminol CEL increases with the increase of ultrasonic power. At the beginning of the reaction, the peak of CEL at 475 nm increased with the increase of time, but the effect of CEL leveled off after the reaction reached 3 h, and there was little difference at 3 h and 5 h, which may be due to the saturation of EDL. Meanwhile, it is found that best CEL was achieved around 40 ℃ with the FEP film in our experiment. The FEP undergoes a glass transition process when the temperature beyond a certain value[32], while the rate of free radicals capture at the reaction site becomes slower at low temperature [33], both leading to diminished CEL intensity.

Furthermore, the surface morphology, elemental composition, and group structures of FEP exhibited no significant changes before and after the CEL reaction, as evidenced by scanning electron microscope (SEM) images, Energy Dispersive Spectrometer (EDS) analysis, fourier transform infrared (FTIR) spectroscopy and X-ray photoelectron spectroscopy (XPS) (**Fig. S13-S15**), further confirming the intrinsic stability of FEP. Specifically, morphological characterization and element mapping of FEP films before and after luminol CEL are reported in **Fig. S13a-b**. No modifications of the morphology were observed by the naked eye and SEM. Besides, the inserted EDS pictures indicated that the composition of FEP remained unchanged. Spectroscopic analysis techniques were also performed to deliver more in-depth information on the chemical properties of FEP films. **Fig. S14** presents FTIR spectroscopy results. The fingerprint region in FTIR characterization, below 1500 cm^{-1}, was stable after the CEL. XPS had been conducted to analyze the variation of the chemical state of FEP films before/after the CEL. The C1s, F1s, and O1s spectra of the FEP films are listed in **Fig. S15a-c**, respectively. Neither shift in binding energies of original peaks nor generation of new peaks was observed after CEL, which further confirmed the chemical stability of FEP. These data indicated that the chemically inert FEP films act as catalysts for the luminol CEL, foreseeing that dielectrics would be reused with very good stability.

Moreover, the concept of CEL, combining CE, CE-Chemistry, and luminescence, has been posited as a universal mechanism. Its effectiveness had been validated in other dielectric materials, including polytetrafluoroethylene (PTFE). As depicted in Fig. 2**g**, the highest luminol luminescence intensity at 475 nm was observed with FEP, followed by PTFE, aligning with the electronegativity and reactivity of ROS generated from the two polymers, respectively. This result encouraged the selection of different dielectric materials to modulate CEL based on the triboelectric series of dielectric materials. It should be noted that the intermediate related to luminol did not always exist stably in the reaction solution. Fig. 2**h** demonstrated a decrease in luminescence intensity at 475 nm and an increase in luminescence intensity at 425 nm within 48 h after the luminol CEL reaction. The HPLC-MS analysis, as illustrated in **Fig. S16**, showed that the concentration of luminol remained consistent with its initial level even after 48 h following the termination of CEL. Although these findings indicated that the intermediate was unstable, its lifespan of hours in the CEL system was still sufficient for detection. This demonstrates the significant contribution of the CEL system to the detection of luminol intermediates and the advancement of research into the luminol mechanism.

3.3. Investigation on the contribution of CE to CEL

According to the generally accepted reaction scheme, a luminol anion is initially oxidized, most probably to radicals, which, depending on the experimental conditions, reacts rapidly with O_2 or hydrogen peroxide to yield a peroxide intermediate [34]. In order to investigate the underlying mechanisms of radical generation and the effect of different additives in different atmospheres on the luminescence of different wavelengths of luminol CEL, N_2 and O_2 were introduced into three kinds of luminol reaction systems, namely systems with xylitol (Fig. 3**a**), with p-benzoquinone (Fig. 3**b**), and with both xylitol and p-benzoquinone (Fig. 3**c**). It could be seen from Fig. 3**a-c** that the luminol luminescence intensity at 425 nm and 475 nm were enhanced by the inclusion of excess O_2. The luminescence intensity at 475 nm was particularly sensitive to O_2, while showing no obvious response under N_2 conditions. A mechanism of radical generation in luminol CEL was proposed in Fig. 3**d**. The frequent growth and collapse of ultrasonication-induced cavitation bubbles maintained periodic contact separation between FEP and DI water [16], leading to the generation of $H_2O\bullet^+$ in DI water through equation (1). Continuous electron transfer from DI water to FEP rendered the FEP negatively charged (FEP*), resulting in the formation of •OH radicals as described in equation (2). During bubble rupture, the released O_2 captured electrons to form $\bullet O_2^-$ radicals, as detailed in equation (3). The generated $\bullet O_2^-$ radicals could react with H_3O^+ to form $HO_2\bullet$ through equation (4). And •OH radicals could be formed by $HO_2\bullet$ through a series of intermediate reactions.

$$H_2O \rightarrow e^- + H_2O\bullet^+ \quad (1)$$

$$H_2O^+ + H_2O \rightarrow \bullet OH + H_3O^+ \quad (2)$$

$$O_2 + FEP\bullet \rightarrow \bullet O_2^- + FEP \quad (3)$$

$$\bullet O_2^- + H_3O^+ \rightarrow HO_2\bullet + H_2O \quad (4)$$

When the excess O_2 was introduced, more $\bullet O_2^-$ radials react with H_3O^+. The protons in the solution were taken away, and the

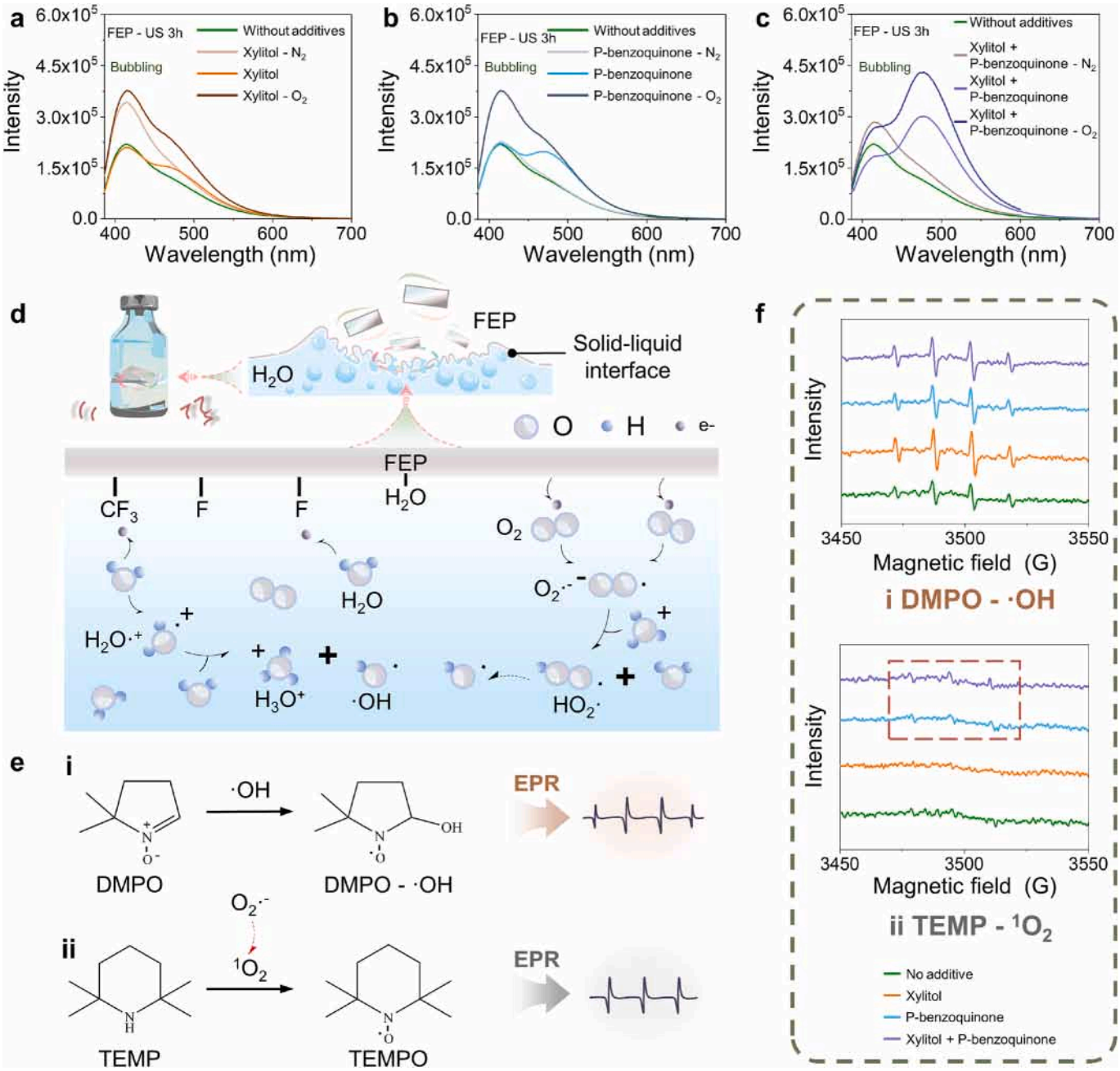

Fig. 3. Investigation on the contribution of radicals to luminol contact-electro-luminescence (CEL). (a-c) Fluorescence spectra of luminol solutions with (a) xylitol, (b) p-benzoquinone, (c) xylitol and p-benzoquinone, respectively, introduced N_2 and O_2. (d) A mechanism of radical generation in luminol CEL. (e) The process of electron paramagnetic resonance (EPR) spectra with 5,5-dimethyl-1-pyrroline N-oxide (DMPO) and 2,2,6,6-tetramethyl-4-piperidone hydrochloride (TEMP) to capture hydroxyl radicals (•OH) and singlet oxygen radicals ($^1O_2$). (f) EPR spectra of DMPO-•OH and TEMP-$^1O_2$ in four different systems.

luminescence peak at 475 nm increased. On the contrary, after the introduction of N_2, less $\bullet O_2^-$ radials were produced, and it could not react with protons, so the luminescence peak at 475 nm decreased. Additionally, the aforementioned equations illustrate that CEL can directly utilize electron transfer at the solid–liquid interface to generate ROS. These ROS can oxidize luminol to form 3-APA* and induce luminescence when the electrons return to 3-APA (ground state) [35–37]. To further understand the energy barriers (ΔE) for realizing CE-induced electron transfer processes of H_2O-FEP, Density Functional Theory (DFT) theoretical calculations of the values of LUMO and HOMO levels for H_2O-FEP in the normal and high pressure were conducted (**Fig. S17**). The ΔE for realizing electron transfer processes between different H_2O and FEP was assessed by DFT, offering a potential explanation for generation of •OH radicals. The DFT parameters and specific calculation method are available in Supplementary Note. To further validate the mechanism, the EPR technique, coupled with the spin trapping agent 5,5-dimethyl-1-pyrroline N-oxide (DMPO) and 2,2,6,6-Tetramethyl-4-piperidone hydrochloride (TEMP) [38], was employed to directly detect radicals in the CE process. As depicted in Fig. 3**e (i)-(ii)**, a characteristic DMPO-OH tetrad peak (1:2:2:1) corresponding to the •OH radicals, and a typical TEMP-$^1O_2$ triplet peak (1:1:1) corresponding to the $^1O_2$ radicals were observed in EPR spectra. Here the $^1O_2$ radicals are generated by the reaction (5) [39,40].

$$\bullet O_2^- + \bullet OH \rightarrow {}^1O_2 + OH^- \quad (5)$$

The •OH radicals were generated in pure NaOH solution, NaOH

solution containing xylitol, NaOH solution containing p-benzoquinone, and NaOH solution containing both xylitol and p-benzoquinone, as evidenced by the typical DMPO-OH tetrad peak (1:2:2:1) appearing in the spectra under US with FEP films shown in Fig. 3**f (i)**. Besides, the presence of $^1O_2$ radicals were detected in the system using TEMP (Fig. 3**f (ii)**), with a typical TEMP-$^1O_2$ triplet peak (1:1:1) appearing on the spectra. The $^1O_2$ radicals were present in the system more obviously only when p-benzoquinone was added, which inferred that the source of $^1O_2$ might be associated with p-benzoquinone. It was reported that $^1O_2$ radicals could enhance the luminol CL reaction [37]. Combined with the foregoing context, it was hypothesized that the introduction of p-benzoquinone might prompt the electron transfer to facilitate the $^1O_2$-induced reaction process. This increase in $^1O_2$ concentration correlates with the enhanced luminescence intensity at 475 nm of luminol in p-benzoquinone-containing solutions. Furthermore, the heightened luminescence observed upon oxygen exposure suggests that p-benzoquinone and oxygen synergistically contribute to $^1O_2$ radical generation during the CEL process. (Fig. 3**b**). To investigate the reasons, DFT was used to calculate the ΔE between FEP and p-benzoquinone with the π^*_{2p} energy level of O_2 under the same condition (**Fig. S18**). The energy level of O_2 molecules matched the LUMO value, while the molecular energy levels of FEP and p-benzoquinone matched the HUMO values of the two systems, respectively. The values of LUMO varied depending on the system. The spatial configurations of FEP/O_2 and p-benzoquinone/O_2 with related DFT modelling source data are in the **Fig. S19**. The results showed that p-benzoquinone-O_2 had lower π^*_{2p} energy level, suggesting that O_2 might react with p-benzoquinone more readily to generate more ROS, thereby enhancing the generation of intermediate.

3.4. Mechanism study of luminol CEL

Based on the previous studies, the mechanism of luminol CEL was proposed as shown in Fig. 4**a**. Luminol lost protons under alkaline aqueous conditions to produce the intermediate product dianion (L^{2-}), which was subsequently catalyzed by ROS generated during the CEL process and then released N_2 to generate the excited state 3-APA* [41]. 3-APA* had two pathways to the ground state 3-APA. One was through the protonation or hydration of process (i), in which it emitted 425 nm luminescence [42]. The other pathway to the ground state involved emitting 475 nm luminescence under deprotonation conditions (process (ii)) such as in aprotic solutions (e.g., dimethyl sulphoxide) [22,43]. Intermediate evidence of luminol ($C_8H_7O_4N$) was detected by HPLC-MS

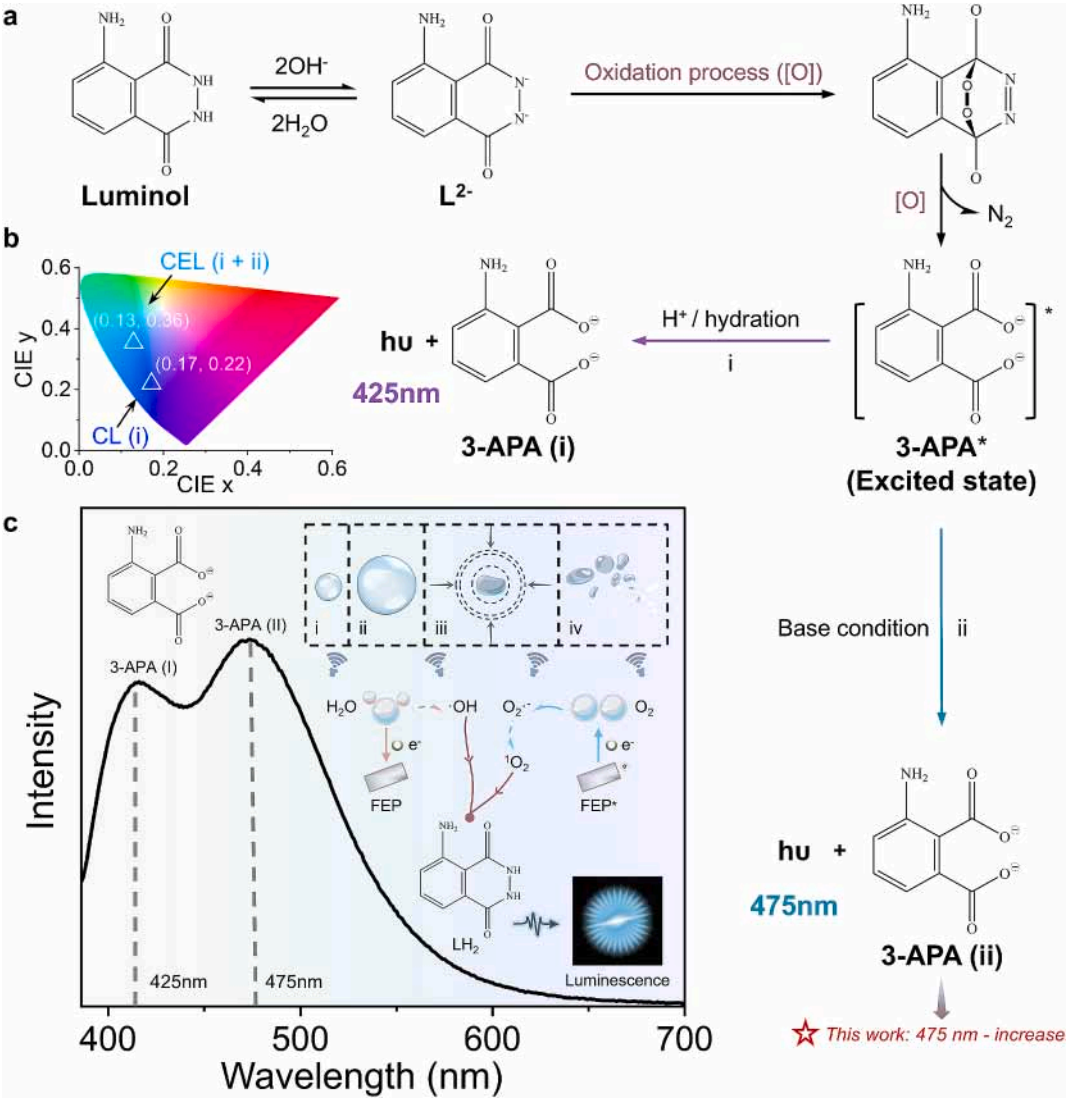

Fig. 4. Mechanism analysis of luminol contact-electro-luminescence (CEL). (a) Contact electrification (CE) induced luminol luminescence through pathways (i) and (ii). Pathway (i) emits light at 425 nm while pathway (ii) emits light at 475 nm. Both wavelengths of light are emitted during the excited state (3-APA*) leaps back to 3-APA. (b) CIE coordinates of CL and CEL of luminol. (c) Complete schematic of luminol CEL. The processes (i) – (iv) upper right corner of the figure represent the formation, growth and collapse of cavitation bubbles provoked by the propagation of ultrasonic waves in solution.

analysis (Fig. S20). The intermediate $C_8H_7O_4N$ consists of two ground states 3-APA (i) and (ii), corresponding to two different pathways (i) and (ii) returning from the excited state 3-APA*. During the competition between the two pathways, the peak at 425 nm produced by process (i) might be reduced in part due to positive hydration of xylitol and proton capture capability of p-benzoquinone, thus enhancing the peak at 475 nm in process (ii). Specifically, positive hydration characteristic of xylitol [29] imposed limitations on the generation of hydrogen bonded 3-APA*, thus promoting the luminol emission peak at 475 nm. The proton-capturing ability of p-benzoquinone likely disrupts the bonding of 3-APA* with H^+ in process (i), thereby favoring process (ii) and resulting in an intensified peak at 475 nm. Furthermore, the fluorescence lifetimes of the emission peaks at 425 nm and 475 nm were assessed before and after the addition of additives. The fluorescence lifetime of luminol at 425 nm remained relatively constant, while that at 475 nm increased (Fig. S21). This suggests an enhanced probability of the excited state 3-APA* returning to the ground state 3-APA via process (ii), underscoring the influence of additives on CEL. Fig. 4**b** showed Commission Internationale de l'Eclairage (CIE) chromaticity diagram of CL and CEL. The luminescence spectrum peak of CL corresponded to CIE coordinates of (0.17, 0.22), while in this work, CEL achieved a luminescence spectrum peak with CIE coordinates of (0.13, 0.36), noting that CEL colour position denoted by the CIE coordinates coincides with the corresponding optical photographs shown in Fig. 1**e**. Generally, the luminescence peak of luminol CL was only observed at 425 nm. However, the CEL approach allowed investigation of specific intermediates, revealing pathways (i) and (ii) that emitted luminescence peaks at 425 nm and 475 nm, respectively. Fig. 4**c** summarized the CEL process. The propagation of ultrasonic waves in solution provoked the formation, growth and collapse of cavitation bubbles as depicted in the processes (i)-(iv) (upper right corner in Fig. 4**c**). Then the collapse of cavitation bubbles might induce frequent CE at the FEP-H_2O interface, leading to electron transfer. The electrons from DI water were transferred to the FEP, and then the O_2 released by the collapse of the bubble took the electrons from the FEP* again. ROS were generated during this process, which could open the ring of luminol and emit luminescence at 425 nm (corresponding to 3-APA (i)) and 475 nm (corresponding to 3-APA (ii)). CEL creates a simple luminescent reaction system that regulates the reaction process and allows the observation of intermediates, offering an effective method for studying the mechanism of the luminol reaction.

4. Conclusions

In summary, this study presents a mild, green and straightforward method of CEL that can utilize the triboelectric charge from CE effect to directly observe the information of the intermediate states of the luminol reaction and regulate the luminescence intensities of the different intermediate states. This method addresses the challenges of creating a pure luminol reaction system within a controllable environment, eliminating side reaction interferences, limitation on electrochemical windows and enabling the observation and control of intermediate processes. Specifically, ultrasonication-triggered frequent contact-separation of FEP-H_2O triggers ROS, which can drive the luminol reaction. The wide versatility of inert solid dielectrics and the ubiquity of the CE effect underscore the universality and simplicity of CEL. In addition, the luminescence intensity of the luminol reaction at 425 nm and 475 nm can be regulated by adding xylitol and p-benzoquinone to the CEL process, which is coupled with the superior spatiotemporal controllability of ultrasonication. Our proposed CEL extends the practicality of ML and establishes a new paradigm based on CE-Chemistry, revealing a simpler approach for green and controllable induction of luminescence reactions and analysis of intermediate processes via CE effects. In the future, CEL will have potential applications in the fields of environmental monitoring and biomedical diagnostics.

CRediT authorship contribution statement

Chong Xu: Writing – review & editing, Writing – original draft, Visualization, Validation, Methodology, Investigation, Formal analysis, Data curation. **Shaoxin Li:** Writing – review & editing, Formal analysis. **Zhe Yang:** Methodology. **Morten Willatzen:** Methodology. **Zhong Lin Wang:** Supervision, Resources, Conceptualization. **Di Wei:** Writing – review & editing, Supervision, Resources, Project administration, Funding acquisition, Formal analysis, Data curation, Conceptualization.

Declaration of competing interest

The authors declare that they have no known competing financial interests or personal relationships that could have appeared to influence the work reported in this paper.

Acknowledgements

We would like to thank Mingming Li, Lixue Yang, Jiajin Liu, and Junhao Wang for their assistance on data measurements. This work was supported by the National Natural Science Foundation (grant number 22479016).

Appendix A. Supplementary data

Supplementary data to this article can be found online at https://doi.org/10.1016/j.cej.2024.157754.

Data availability

Data will be made available on request.

References

[1] F. Barni, S.W. Lewis, A. Berti, G.M. Miskelly, G. Lago, Forensic application of the luminol reaction as a presumptive test for latent blood detection, Talanta 72 (2007) 896–913.
[2] P. Khan, D. Idrees, M.A. Moxley, J.A. Corbett, F. Ahmad, G. von Figura, W.S. Sly, A. Waheed, M.I. Hassan, Luminol-Based Chemiluminescent Signals: Clinical and Non-clinical Application and Future Uses, Appl. Biochem. Biotechnol. 173 (2014) 333–355.
[3] J. Lind, G. Merényi, Determination of the chemiluminescence quantum yield of luminol in rapid chemical reactions, Chem. Phys. Lett. 82 (1981) 331–334.
[4] X. Zhang, W. Lu, C. Ma, T. Wang, J.-J. Zhu, R.N. Zare, Q. Min, Insights into electrochemiluminescence dynamics by synchronizing real-time electrical, luminescence, and mass spectrometric measurements, Chem. Sci. 13 (2022) 6244–6253.
[5] H. Zhang, Y. Wei, X. Huang, W. Huang, Recent development of elastico-mechanoluminescent phosphors, J. Lumin. 207 (2019) 137–148.
[6] T. Miura, M. Chini, R. Bennewitz, Forces, charges, and light emission during the rupture of adhesive contacts, J. Appl. Phys. 102 (2007) 103509.
[7] C. Wang, H. Hu, D. Peng, L. Dong, D. Zhu, Soft devices empowered by mechanoluminescent materials, Soft Science 3 (2023) 39.
[8] Y. Wang, Z. Yi, J. Guo, S. Liao, Z. Li, S. Xu, B. Yin, Y. Liu, Y. Feng, Q. Rong, X. Liu, G. Song, X.-B. Zhang, W. Tan, In vivo ultrasound-induced luminescence molecular imaging, Nat. Photonics 18 (2024) 334–343.
[9] M.P. Brenner, S. Hilgenfeldt, D. Lohse, Single-bubble sonoluminescence, Rev. Mod. Phys. 74 (2002) 425–484.
[10] S. Daniels, D.J. Price, Sonoluminescence in water and agar gels during irradiation with 0.75 mhz continuous-wave ultrasound, Ultrasound Med. Biol. 17 (1991) 297–308.
[11] N.A. Atari, Piezoluminescence phenomenon, Phys. Lett. A 90 (1982) 93–96.
[12] Y. Zhuang, X. Li, F. Lin, C. Chen, Z. Wu, H. Luo, L. Jin, R.J. Xie, Visualizing Dynamic Mechanical Actions with High Sensitivity and High Resolution by Near-Distance Mechanoluminescence Imaging, Adv. Mater. 34 (2022) 2202864.
[13] Y. Xie, Z. Li, Triboluminescence: Recalling Interest and New Aspects, Chem 4 (2018) 943–971.
[14] W. Wang, Z. Wang, J. Zhang, J. Zhou, W. Dong, Y. Wang, Contact electrification induced mechanoluminescence, Nano Energy 94 (2022) 106920.
[15] L. Su, H. Wang, Y. Zi, Recent progress of triboelectrification-induced electroluminescence: from fundaments to applications, Journal of Physics: Materials 4 (2021) 042001.
[16] Z. Wang, A. Berbille, Y. Feng, S. Li, L. Zhu, W. Tang, Z.L. Wang, Contact-electro-catalysis for the degradation of organic pollutants using pristine dielectric powders, Nat. Commun. 13 (2022) 130.

[17] Z. Wang, X. Dong, X.-F. Li, Y. Feng, S. Li, W. Tang, Z.L. Wang, A contact-electro-catalysis process for producing reactive oxygen species by ball milling of triboelectric materials, Nat. Commun. 15 (2024) 757.
[18] A. Berbille, X.F. Li, Y. Su, S. Li, X. Zhao, L. Zhu, Z.L. Wang, Mechanism for Generating H_2O_2 at Water-Solid Interface by Contact-Electrification, Adv. Mater. 35 (2023) 2304387.
[19] H. Li, A. Berbille, X. Zhao, Z. Wang, W. Tang, Z.L. Wang, A contact-electro-catalytic cathode recycling method for spent lithium-ion batteries, Nature Energy 8 (2023) 1137–1144.
[20] Y. Su, A. Berbille, X.-F. Li, J. Zhang, M. PourhosseiniAsl, H. Li, Z. Liu, S. Li, J. Liu, L. Zhu, Z.L. Wang, Reduction of precious metal ions in aqueous solutions by contact-electro-catalysis, Nat. Commun. 15 (2024) 4196.
[21] S. Li, Z. Zhang, P. Peng, X. Li, Z.L. Wang, D. Wei, A green approach to induce and steer chemical reactions using inert solid dielectrics, Nano Energy 122 (2024) 109286.
[22] S. Hirsch, S. Speiser, Concentration effects in the chemiluminescence of luminol, J. Photochem. 10 (1979) 159–162.
[23] S. Lin, X. Chen, Z.L. Wang, Electron transfer in liquid–solid contact electrification and double-layer formation, in: Reference Module in Chemistry, Molecular Sciences and Chemical Engineering, 2023, pp. 576-599.
[24] Z. Wang, X. Dong, W. Tang, Z.L. Wang, Contact-electro-catalysis (CEC), Chem. Soc. Rev. 53 (2024) 4349–4373.
[25] D. Yoo, S. Jang, S. Cho, D. Choi, D.S. Kim, A Liquid Triboelectric Series, Adv. Mater. 35 (2023) 2300699.
[26] M. Carlevaro, E.R. Caffarena, J.R. Grigera, Hydration properties of xylitol: computer simulation, Int. J. Biol. Macromol. 23 (1998) 149–155.
[27] C.A. Walker, Photochemistry in the liquid and solid states, L. J. Heidt, R. S. Livingston, E. Rabinowitch, and Farrington Daniels, editors, John Wiley and Sons, New York, New York. 174 pages, AIChE Journal, 8 (2004) 431-431.
[28] E.H. White, M.M. Bursey, Chemiluminescence of LUminol and Related Hydrazides: The Light Emission Step, J. Am. Chem. Soc. 86 (2002) 941–942.
[29] E. Howard, J.R. Grigera, Conformations of erythritol and L-threitol in aqueous solution in relation to sweetness properties: a molecular dynamics simulation, J. Chem. Soc. Faraday Trans. 88 (1992) 437–441.
[30] J.R. Grigera, Conformation of polyols in water. Molecular-dynamics simulation of mannitol and sorbitol, J. Chem. Soc., Faraday Trans. 1 84 (1988) 2603–2608.
[31] H.S. Isbell, H.L. Frush, Mechanisms for hydroperoxide degradation of disaccharides and related compounds, Carbohydr. Res. 161 (1987) 181–193.
[32] X. Dong, Z. Wang, A. Berbille, X. Zhao, W. Tang, Z.L. Wang, Investigations on the contact-electro-catalysis under various ultrasonic conditions and using different electrification particles, Nano Energy 99 (2022).
[33] B. Mile, Free Radical Studies at Low Temperatures, Angew. Chem. Int. Ed. Eng. 7 (2003) 507–519.
[34] K.E. Haapakka, J.J. Kankare, The mechanism of the electrogenerated chemiluminescence of luminol in aqueous alkaline solution, Anal. Chim. Acta 138 (1982) 263–275.
[35] G. Merenyi, J. Lind, T.E. Eriksen, The Reactivity Of Superoxide (O_2^-) and its ability to induce chemiluminescence with luminol, Photochem. Photobiol. 41 (2008) 203–208.
[36] G. Periyasami, L. Martelo, C. Baleizão, M.N. Berberan-Santos, Strong green chemiluminescence from naphthalene analogues of luminol, New J. Chem. 38 (2014) 2258.
[37] D.M. Wang, Y. Zhang, L.L. Zheng, X.X. Yang, Y. Wang, C.Z. Huang, Singlet Oxygen Involved Luminol Chemiluminescence Catalyzed by Graphene Oxide, J. Phys. Chem. C 116 (2012) 21622–21628.
[38] G. Nardi, I. Manet, S. Monti, M.A. Miranda, V. Lhiaubet-Vallet, Scope and limitations of the TEMPO/EPR method for singlet oxygen detection: the misleading role of electron transfer, Free Radic. Biol. Med. 77 (2014) 64–70.
[39] X. Dou, Z. Lin, H. Chen, Y. Zheng, C. Lu, J.-M. Lin, Production of superoxide anion radicals as evidence for carbon nanodots acting as electron donors by the chemiluminescence method, Chem. Commun. 49 (2013) 5871.
[40] J.-M. Lin, M. Liu, Chemiluminescence from the Decomposition of Peroxymonocarbonate Catalyzed by Gold Nanoparticles, J. Phys. Chem. B 112 (2008) 7850–7855.
[41] C.D. Kalkar, H.J. Arnikar, S.V. Doshi, R.S. Varkhede, Mechanism of aqualuminescence in alkaline lumimol, Int. J. Appl. Radiat. Isot. 36 (1985) 51–55.
[42] E.H. White, O. Zafiriou, H.H. Kagi, J.H.M. Hill, Chemilunimescence of Luminol: The Chemcial Reaction, J. Am. Chem. Soc. 86 (2002) 940–941.
[43] V.S. Butt, Light and Life, Nature 192 (1961) 296.